First-principles calculations of the vibrational spectra of one-dimensional C_{60} polymers

Titus A. Beu*
Faculty of Physics, University "Babeş-Bolyai," 3400 Cluj-Napoca, Romania

Jun Onoe
Research Laboratory for Nuclear Reactors, Tokyo Institute of Technology, 2-12-1 O-okayama, Tokyo 152-8550

(Received 24 August 2006; revised manuscript received 4 October 2006; published 20 November 2006)

The vibrational properties of several C_{60} dimers belonging to the Stone-Wales rearrangement sequence [described by E. Osawa and K. Honda, Full. Sci. Technol. **4**, 939 (1996)], along with a trimer and a tetramer isomer are investigated by tight-binding and density functional calculations. The IR absorption bands found by Onoe, Nakayama, Aono and Hara [Appl. Phys. Lett. **82**, 595 (2003)] in the spectra of electron-beam irradiated C_{60} films are explained and attributed mainly to surface vibrations located in the waist region of the considered polymers. The features of the Raman spectra are also discussed and related to experimental spectra of photopolymerized C_{60}.

DOI: 10.1103/PhysRevB.74.195426 PACS number(s): 71.15.Mb, 71.20.Tx

I. INTRODUCTION

The polymerization of C_{60} induced by electron-beam (EB) irradiation has proven to be a viable technique for nanofabrication of C_{60}-based carbon materials, potentially useful for developing carbon-based nanodevices. Onoe and others have extensively investigated EB polymerized C_{60} films by *in situ* Fourier-transform infrared spectroscopy, *in situ* x-ray photoelectron spectroscopy, and *in situ* scanning tunneling microscopy.[1–5] In EB polymerized films, C_{60} molecules coalesce to form tubular linkages and the metallic-type resistivity, found by *ex situ* four-probe measurements to be as low as 7 Ω cm, is considerably smaller than that of the insulating solid C_{60} (10^8–10^{14} Ω cm).[3]

The measured IR spectra show that as polymerization proceeds, supplementary peaks develop around 1340, 1360, and 1390 cm^{-1} as compared to the pristine C_{60} film.[2–4] Vibrational calculations based on the AM1 semiempirical method have been carried out by Hara and Onoe for several peanut-shaped C_{120} isomers.[4] Qualitatively, the results have evidenced that the IR absorption band observed in the range 1300–1400 cm^{-1} can be attributed to the normal modes involving mainly atomic in-plane motions located in the waist region. Earlier, very interesting density-functional tight-binding calculations of vibrational properties of C_{60} oligomers have been published by Porezag and Fravenheim[6]

The present investigations are primarily intended to explain in more detail the observed IR spectra of EB irradiated C_{60} films by means of calculations of vibrational properties of one-dimensional C_{60} polymers. The described calculations are a sequel to the previously published work concerning the electronic structure of one-dimensional C_{60} polymers,[7] aimed at explaining the metallic behavior of EB irradiated films and providing the structural data. Both the present and the previous research rely on two complementary approaches: (a) efficient tight-binding (TB) parametrizations and (b) all-electron density functional theory (DFT) with carefully assessed exchange-correlation functionals.

Since the computational effort required to obtain IR and, in particular, Raman spectra for C_{120} peanuts lacking any exploitable symmetry properties is a real challenge even for up-to-date machines, our vibrational DFT calculations are limited to the only isomer of the Stone-Wales rearrangement path (besides the capped nanotube), which shows any symmetry at all, i.e., the C_{2h}-symmetry peanut designated in our previous paper as P4. Not being subject to such constraints, the TB calculations are feasible in reasonable amounts of time for larger polymers, as such we have investigated several of the Stone-Wales C_{120} isomers, along with the trimer (C_{180}) and tetramer (C_{240}) derived from P4. The vibrational TB and DFT results turn out to be consistent, offering a truthful explanation of the observed vibrational spectra.

II. CALCULATION METHODS

We have successfully employed the TB method over the last years for describing structural and vibrational properties of the C_{36}, C_{60}, and C_{70} fullerenes.[7–9] The TB approaches can be viewed as simplified two-center-oriented *ab initio* methods, with the electronic properties calculated from a parametrized representation of the Kohn-Sham equation. The TB parametrization of Papaconstantopoulos *et al.*[10] describes the environment of each atom by a pseudo-atomic density,

$$\rho_I = \sum_{J \neq I}^{N} \exp(-\lambda^2 R_{IJ}) f(R_{IJ}),$$

which depends exponentially on the distances to all neighbors and features a cutoff function

TABLE I. HOMO-LUMO gap Δ and (longitudinal) extents L of C_{60} and its dimer P4 obtained from DFT calculations with the basis sets 6–31 g(d) and 6–31 g, respectively. The differences between the basis sets are indicated in parentheses.

	Basis set	Δ (eV)	L (Å)
C_{60}	6–31 g(d)	1.668	6.987
	6–31 g	1.770 (0.10)	7.013 (0.03)
C_{120} (P4)	6–31 g(d)	0.333	15.99
	6–31 g	0.379 (0.05)	16.04 (0.05)

TABLE II. Frequencies and intensities (activities) of the IR and Raman active vibrational modes of C_{60} resulted from DFT calculations and experiment.

	6–31 g(d)		6–31 g		Exp.	
T_{1u}	513	22.3	527	21.2	527[a]	1.00
T_{1u}	577	11.9	575	10.2	576[a]	0.30
T_{1u}	1193	8.8	1186	9.91	1183[a]	0.22
T_{1u}	1447	9.2	1464	14.2	1429[a]	0.24
A_g	488	143	487	138	493[b]	0.02
A_g	1487	312	1506	365	1468[b]	0.10
H_g	257	24.2	262	23.9	270[b]	0.52
H_g	419	0.27	430	0.43	430[b]	0.40
H_g	686	0.27	700	0.44	708[b]	0.40
H_g	771	8.68	771	7.55	772[b]	0.38
H_g	1101	11.4	1103	11.6	1099[b]	0.01
H_g	1255	18.1	1250	20.6	1248[b]	0.01
H_g	1435	2.35	1445	2.95	1426[b]	0.44
H_g	1570	47.1	1581	52.0	1573[b]	0.52

[a]Reference 19.
[b]Reference 20.

$$f(R) = \frac{1}{1 + \exp[(R - R_c)/\Delta]}.$$

The parameters employed for carbon are $R_c = 10.5\ a_0$ and $\Delta = 0.5\ a_0$ (a_0 is the Bohr radius).

The (diagonal) *on-site* Hamiltonian elements are parametrized in terms of the local pseudoatomic density by

$$h_l^I = \alpha_l + \beta_l \rho_I^{2/3} + \gamma_l \rho_I^{4/3} + \chi_l \rho_I^2,$$

where $l = s, p$. The two-center Slater-Koster hopping terms are defined as polynomials with an exponential cutoff ($\mu = \sigma, \pi$)

$$H_{ll'\mu}(R) = (a_{ll'\mu} + b_{ll'\mu} R + c_{ll'\mu} R^2) \exp(-d_{ll'\mu}^2 R) f(R)$$

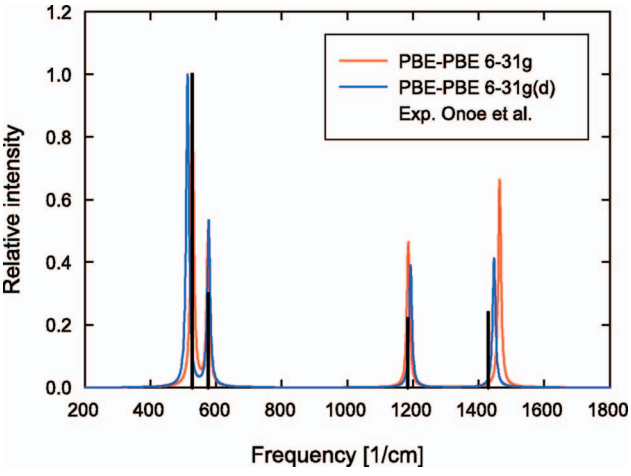

FIG. 1. (Color) IR-spectrum of the C_{60} fullerene resulted from DFT calculations with the PBE-PBE exchange-correlation functional and the 6–31 g and 6–31 g(d) basis sets, along with the experimental results of Onoe *et al.*[3,5] (drop lines).

$$S_{ll'\mu}(R) = (\delta_{ll'} + p_{ll'\mu} R + q_{ll'\mu} R^2 + r_{ll'\mu} R^3) \times \exp(-s_{ll'\mu}^2 R) f(R).$$

The approach we used to analyze the vibrational properties within the harmonic approximation is based on the dynamical matrix.[11] For this approach to be applicable, one has to start from a fully relaxed geometrical structure of the molecular aggregate under consideration. The elements of the dynamical matrix have the significance of local curvatures of the potential energy surface at the atom sites, and they can be approximated by

$$\mathcal{H}_{IJ}^{\alpha\beta} = -\frac{F_I^\alpha(r_J^\beta + h) - F_I^\alpha(r_J^\beta - h)}{2h} + O(h^2),$$

$$I, J = 1, 2, \ldots, N, \quad \alpha, \beta = x, y, z,$$

$F_I^\alpha(r_J^\beta \pm h)$ being the α component of the force acting on atom I when atom J is displaced by $\pm h$ along direction β.

In order to obtain the vibrational frequencies and the corresponding atomic displacements for the normal modes, one has to solve then the generalized eigenvalue problem for the dynamical matrix

$$\mathcal{H} \cdot \delta \mathbf{r}_k = \omega_k^2 \mathbf{M} \cdot \delta \mathbf{r}_k, \quad k = 1, 2, \ldots, 3N.$$

Here, ω_k is the eigenvalue (frequency) of normal mode k, $\delta \mathbf{r}_k$ is the corresponding eigenvector (having as components the atomic displacements), and $\mathbf{M}$ is the diagonal matrix with the atomic masses on the main diagonal.

Our DFT calculations have been carried out using the package GAUSSIAN 03.[12] In our previous paper,[7] we have provided evidence for the superiority of two recent functionals in calculations regarding fullerenes as compared to the traditional B3LYP functional.[13] The employed PBE exchange and, respectively, gradient-corrected correlation func-

TABLE III. TB vibrational results for several C_{60} peanuts belonging to the Stone-Wales rearrangement pathway, and for the trimer and tetramer derived from the P4 peanut. Only the three most intense lines between 1300 and 1400 cm^{-1} are included for each species. Δ designates the HOMO-LUMO gap and I is the IR intensity.

Δ (eV)	ν	I	sym.	Δ (eV)	ν	I	sym.	Δ (eV)	ν	I	sym.
	P4				P7				P8		
0.294	1317	0.05	A_u	0.587	1317	0.06	A	0.370	1300	0.17	A
	1333	0.06	E_u		1338	0.08	A		1333	0.06	A
	1381	0.16	E_u		1375	0.11	A		1379	0.13	A
	P12				P16				P20		
0.273	1316	0.20	A	0.256	1302	0.05	A	0.184	1302	0.04	A
	1340	0.10	A		1322	0.05	A		1315	0.04	A
	1389	0.05	E		1338	0.06	A		1357	0.03	A
	P24				C_{180}				C_{240}		
0.566	1314	0.06	E_u	0.050	1317	0.03	A_u	0.195	1363	0.05	A_u
	1379	0.17	E_u		1382	0.17	A_u		1380	0.12	E_u
	1399	0.17	E_u		1392	0.01	E_u		1389	0.02	A_u

tionals of Perdew *et al.*,[14] and the HCTH exchange functional including gradient-corrected correlation of Hamprecht *et al.*[15] reproduce fairly the experimental HOMO-LUMO gap of C_{60} (1.6–1.85 eV.),[16] i.e., 1.668 eV (PBE), and 1.698 eV (HCTH). In the present work, we have used only the PBE functional, the corresponding results yielded by the HCTH functional being insignificantly different.

Since all-electron DFT calculations of the IR and Raman spectra of C_{60} dimers employing the split valence polarized basis set 6–31 g(d) (used throughout in our previous paper) have turned out to involve excessive computer resources, we have performed all production calculations reported here using the subset 6–31 g. A comparison of the accuracy of the structural results provided by the two basis sets is given in Table I, with regard to the HOMO-LUMO gap and the geometrical extents of C_{60} and its dimer P4. Although the relative differences between the 6–31 g and the 6–31 g(d) results reach as much as 12.1% for the HOMO-LUMO gap in the case of the P4 dimer (0.05 eV), the geometrical extents coincide within <0.4% (0.05 Å).

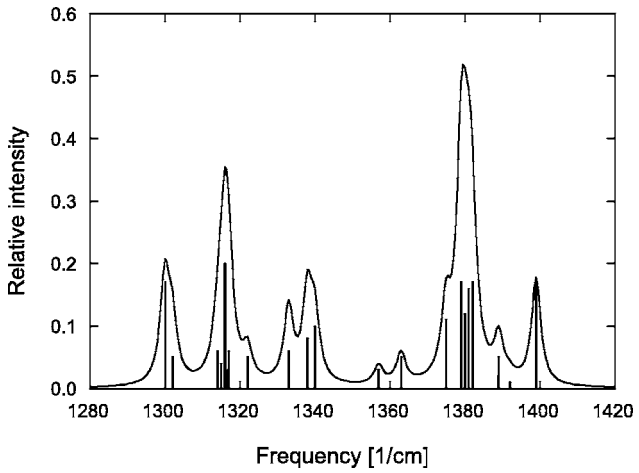

FIG. 2. IR-lines for the peanuts P4, P7, P8, P12, P16, P20, and P24 and convoluted spectrum of corresponding Lorentzian peaks resulted from TB calculations.

In order to assess the way the two basis sets perform in spectroscopy applications, we have carried out also preliminary calculations regarding the vibrational modes of C_{60}. The comparison of the calculated and experimental frequencies (Table II) emphasizes a rather reassuring aspect: as compared to the 6–31 g(d) basis set, the 6–31 g subset seems to reproduce equally well three of the four IR-active modes (T_{1u} symmetry) and five of the ten Raman-active modes (A_g and H_g symmetry).

It is a matter of common knowledge that first-principles methods typically tend to overestimate the vibrational frequencies (by up to 10%), mainly due to inherent approximations in the electron correlation, and DFT methods are no exception to this behavior.[17] It should be noted, however, that we employed no scaling and that all frequencies of C_{60} were reproduced within <3%. For the lowest three IR active modes, the absolute deviations do not exceed 4 cm^{-1}.

The reasonable deviations with respect to the experiment caused by the smaller 6–31 g basis set, obtained nevertheless at a significantly lower computational effort, can be judged also visually from Fig. 1, where the measurements of Hara *et al.*,[1] represented as drop lines, are used as reference.

III. RESULTS AND DISCUSSION

Seven of the nine C_{60} polymers investigated in this study are dimers belonging to the Stone-Wales rearrangement sequence, described by Osawa and Honda [18] and characterized by the fact that the interconversion between successive isomers can be achieved merely by rotations of atom pairs about their bond center. The dimers considered here are namely P4, P7, P8, P12, P16, P20, and the capped nanotube P24. Only four of all polymers show well-defined symmetry: the P4 peanut, along with the trimer (C_{180}) and the tetramer (C_{240}) derived from it have C_{2h} symmetry, while the P24

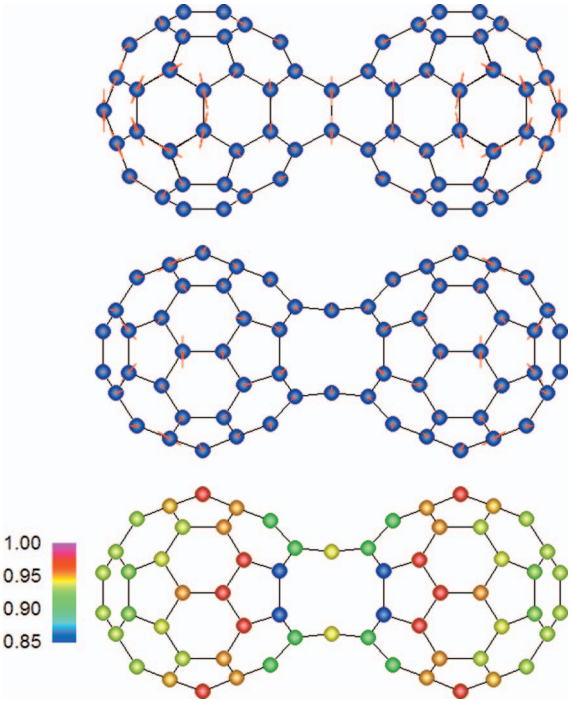

FIG. 3. (Color) Atomic displacements for the IR-active vibrational mode at 1333 cm^{-1} and pseudoatomic density for the P4 peanut yielded by TB calculations.

nanotube shows C_5 symmetry. The geometrical structure of all polymers was optimized corresponding to the tight-binding force field by simulated annealing embedded in molecular dynamics.

Table III summarizes all relevant TB results for the considered polymers. Besides the HOMO-LUMO gap, the frequency, intensity and symmetry of the three most intense IR-active modes located in the interval 1300–1400 cm^{-1} (where the major changes in the electron-beam irradiated C_{60} films were observed) are listed for each isomer. Because of their symmetry properties, the P4 and the P24 peanuts, together with the trimer and tetramer derived from P4, feature *ungerade* IR-active vibrations. As general findings, all structures investigated possess at TB level IR lines in the interval 1300–1400 cm^{-1} and the most intense vibrations are predominantly surface modes.

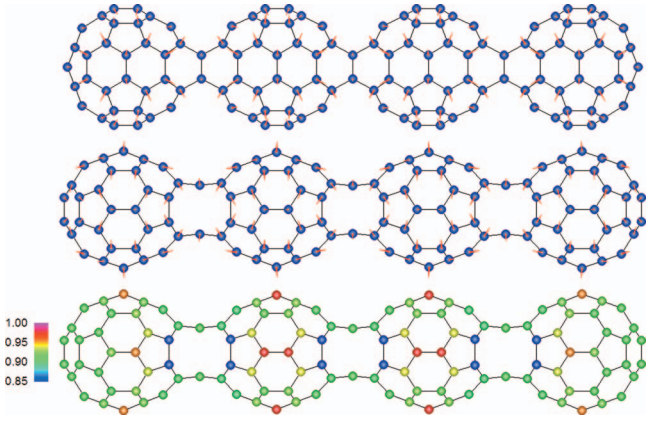

FIG. 4. (Color) Atomic displacements for the IR-active vibrational mode at 1380 cm^{-1} and pseudoatomic density for the tetramer derived from the P4 peanut, yielded by TB calculations.

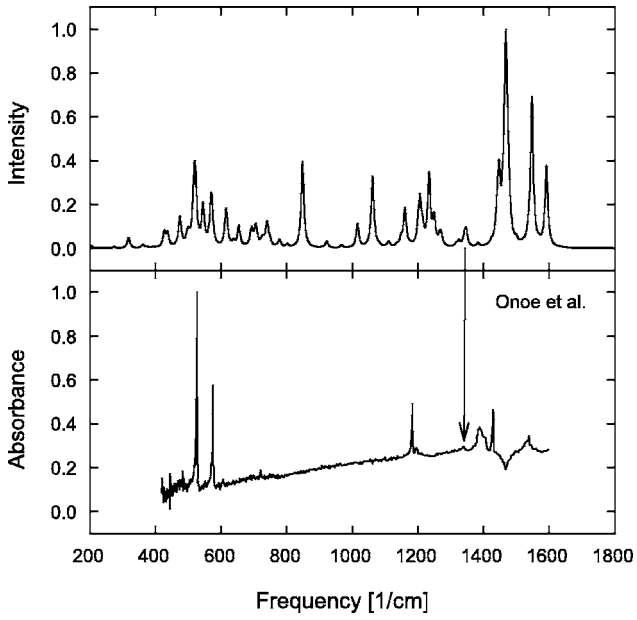

FIG. 5. IR spectrum of the P4 peanut obtained from DFT calculations with the PBE-PBE exchange-correlation functional and the 6–31 g basis set, along with the experimental spectrum of Onoe *et al.*[1]

Even though there are no obvious correlations between the position of the peanuts in the Stone-Wales sequence and the frequency, intensity, or symmetry of their vibrations, Fig. 2, where the convoluted spectrum of all investigated polymers is depicted, clearly shows that more intense bands are formed around 1320, 1340, and 1380 cm^{-1}. The convoluted spectrum was obtained by assigning Lorentzian peaks of half width 1 cm^{-1} to the calculated TB frequencies and, by a small rescaling of 0.98, this spectrum provides a consistent explanation of the experimental spectrum. For the bands around 1320 and 1340 cm^{-1}, the P12 peanut, located just in the middle of the Stone-Wales rearrangement pathway, seems to be mainly responsible. The experimental absorption

TABLE IV. IR active vibrational modes of the peanut P4 in the interval 1300–1400 cm^{-1} obtained with the PBE-PBE exchange-correlation functional and the 6–31 g basis set.

ν	IR intensity	symmetry
1307.08	0.14	A_u
1316.11	0.83	B_u
1316.67	1.05	B_u
1324.68	3.62	A_u
1331.55	0.40	B_u
1341.56	2.79	B_u
1342.26	4.31	B_u
1347.16	9.43	A_u
1382.83	2.39	B_u

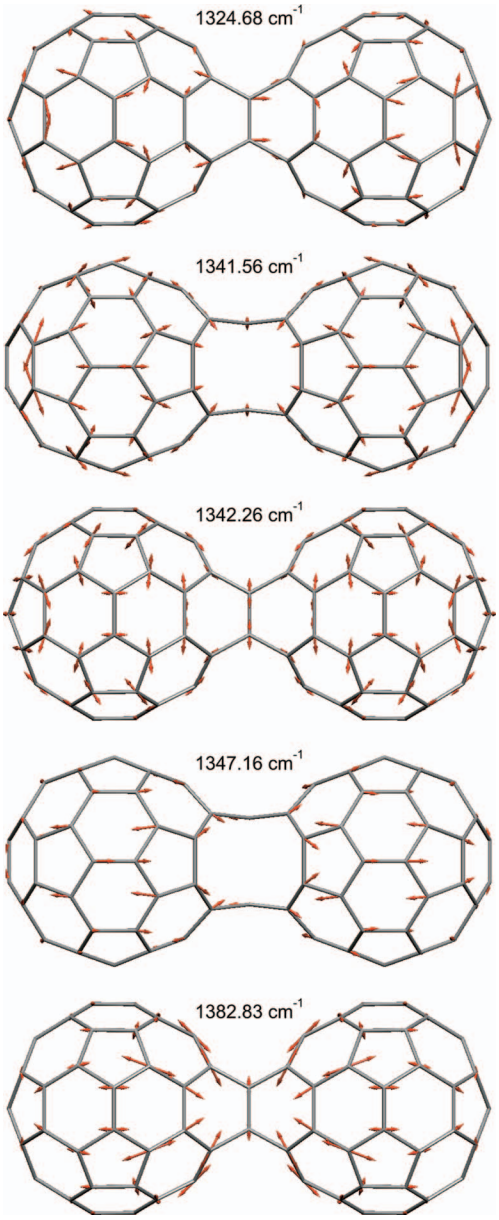

FIG. 6. (Color) Most intense IR-active vibrational modes of the P4 peanut between 1300 and 1400 cm^{-1} yielded by DFT calculations with the exchange-correlation functional PBE-PBE and the 6–31 g basis set.

maximum (~1380 cm^{-1}) can be well explained especially by the small peanuts (up to P8 and including the polymers derived from the symmetric peanut P4).

Since visualizing normal vibrations of molecular structures without symmetry properties is inherently difficult, we have chosen to illustrate the TB results by normal modes of the P4 peanut (Fig. 3) and of the tetramer derived from P4 (Fig. 4). Both normal modes are located in the interval of interest (between 1300 and 1400 cm^{-1}). The vibration of the P4 peanut located at 1333 cm^{-1} is seen to be predominantly a surface mode involving mainly the longitudinal belt of hexagons comprising the waist region (upper view). The pseudoatomic density reaches its minimum (blue) at atomic sites located in the waist region. The normal mode of the

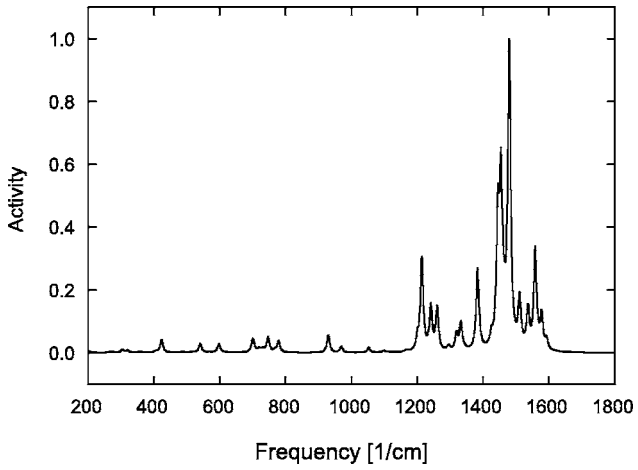

FIG. 7. Raman spectrum of the P4 fullerene obtained from DFT calculations with the exchange-correlation functional PBE-PBE and the basis set 6–31 g.

tetramer derived from P4 is also largely a surface mode, with low pseudoatomic density in the waist regions.

As already pointed out, our DFT calculations have been carried out employing the PBE-PBE exchange-correlation functional of Perdew *et al.*[14] and, for feasibility reasons, the 6–31 g basis set, which has proven to provide vibrational results of comparable quality with the larger 6–31 g(d) basis set. The calculations have been limited to the P4 peanut, whose symmetry properties can be exploited in reducing significantly the computation time.

Figure 5 shows the calculated IR spectrum (without any scaling), along with the experimental spectrum of an electron-beam irradiated C_{60} film on a CsI substrate published by Onoe *et al.*[1] It is easily noticeable that the experimental absorption peak developing around 1340 cm^{-1} as a consequence of the electron-beam irradiation has a matching peak in the calculated spectrum (the two peaks are connected by an arrow). Besides the fair agreement of the DFT and TB results concerning the existence of a peak around 1340 cm^{-1}, the symmetric P4 peanut alone offers already an explanation of the IR behavior of the coalesced structures formed by electron-beam irradiation.

As can be seen from Table IV, where the normal modes with the frequency comprised between 1300 and 1400 cm^{-1} have been listed, the most intense IR-active mode is located at 1347 cm^{-1}, having A_u symmetry and more than the double intensity as compared to the rest of the normal modes. Moreover, having in view only the five most intense modes, it is

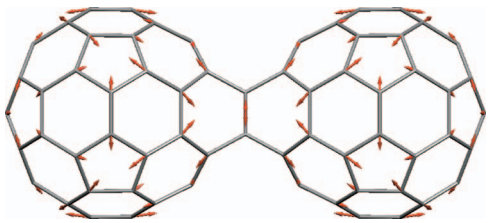

FIG. 8. (Color) Raman-active vibrational mode of the P4 peanut at 1510.76 cm^{-1} corresponding to the $A_g(2)$ pinch mode of the C_{60} fullerene located at 1469 cm^{-1}.

interesting to note that the DFT calculations on the P4 peanut confirm the appearance of three groups of IR-active modes (already suggested by the TB results), located, respectively, around 1320, 1340, and 1380 cm^{-1}.

Figure 6 shows the displacement patterns of the five most intense IR-active modes, and these appear to be predominantly surface modes. In particular, the most intense mode at 1347 cm^{-1} is predominantly a *longitudinal* surface mode. The surface character of the most intense modes is again in agreement with the TB findings, holding also for the rest of the considered polymers.

Even though no Raman spectra for electron-beam irradiated C_{60} films are available in the literature, we have depicted in Fig. 7 the Raman spectrum resulted for the P4 peanut by our DFT calculations. The most significant Raman-activity occurs between 1200 and 1600 cm^{-1}. The most pronounced peak appears at 1479 cm^{-1}, in the range of the $A_g(2)$ pinch mode of pristine C_{60} (located at 1469 cm^{-1}). However, the normal mode corresponding to the C_{60} pinch mode is actually the one located at 1510 cm^{-1} and its displacement pattern can be seen in Fig. 8. Applying the scaling factor 0.975 suggested by the calculations for C_{60} (see Table II), the "pinch" mode of the P4 peanut repositions at 1473 cm^{-1}, which overestimates by $<0.7\%$ the measurements of Burger *et al.*[21] on photopolymerized C_{60}.

It should be noted that the scaling applied to our Raman spectrum is comprised within the range commonly considered to be moderate (0.95–1), Raman spectra being known to be particularly sensitive to the employed combination of basis set and exchange-correlation functional.[17]

As suggested by the results for C_{60}, the basis set 6–31 g(d) would perform better in the particular case of the Raman spectrum.

IV. CONCLUSIONS

The vibrational properties of several one-dimensional C_{60} polymers have been investigated by tight-binding and density functional theory calculations. Both approaches provide a consistent explanation of the measured IR-spectra of electron-beam irradiated C_{60} films, mainly, the existence of a significant absorption maximum around 1340 cm^{-1}. Additional peaks are predicted by both approaches around 1320 and 1380 cm^{-1}. The most intense IR-active vibrational modes between 1300 and 1400 cm^{-1} have been found to be predominantly surface modes. By slight scaling, the DFT calculations reproduce the features developing in the Raman spectra of photopolymerized C_{60}.

ACKNOWLEDGMENT

One of the authors (T.A.B.) gratefully acknowledges a visiting professor position at the Tokyo Institute of Technology.

*Electronic address: tbeu@phys.ubbcluj.ro

[1] T. Hara, J. Onoe, H. Tanaka, Y. Li, and K. Takeuchi, Jpn. J. Appl. Phys., Part 1 **39**, 1872 (2000).
[2] T. Hara, J. Onoe, and K. Takeuchi, J. Appl. Phys. **92**, 7302 (2002).
[3] J. Onoe, T. Nakayama, M. Aono, and T. Hara, Appl. Phys. Lett. **82**, 595 (2003).
[4] T. Hara and J. Onoe, Eur. Phys. J. D **24**, 389 (2003).
[5] J. Onoe, T. Nakayama, M. Aono, and T. Hara, J. Phys. Chem. Solids **65**, 343 (2004).
[6] D. Porezag and T. Frauenheim, Carbon **37**, 463 (1999).
[7] T. A. Beu, J. Onoe, and A. Hida, Phys. Rev. B **72**, 155416 (2005).
[8] T. A. Beu, J. Onoe, and K. Takeuchi, Eur. Phys. J. D **10**, 391 (2000).
[9] T. A. Beu, J. Onoe, and K. Takeuchi, Eur. Phys. J. D **17**, 205 (2001).
[10] D. A. Papaconstantopoulos, M. J. Mehl, S. C. Erwin, and M. R. Pederson, in *Tight-Binding Approach to Computational Materials Science*, edited by P. Turchi, A. Gonis, and L. Colombo, MRS Symposia Proceedings No. 491 (Materials Research Society, Warendale, PA, 1998), p. 221.
[11] Th. Köhler, Th. Frauenheim, and G. Jungnickel, Phys. Rev. B **52**, 11837 (1995).
[12] M. J. Frisch, G. W. Trucks, H. B. Schlegel, G. E. Scuseria, M. A. Robb, J. R. Cheeseman, J. A. Montgomery, Jr., T. Vreven, K. N. Kudin, J. C. Burant, J. M. Millam, S. S. Iyengar, J. Tomasi, V. Barone, B. Mennucci, M. Cossi, G. Scalmani, N. Rega, G. A. Petersson, H. Nakatsuji, M. Hada, M. Ehara, K. Toyota, R. Fukuda, J. Hasegawa, M. Ishida, T. Nakajima, Y. Honda, O. Kitao, H. Nakai, M. Klene, X. Li, J. E. Knox, H. P. Hratchian, J. B. Cross, C. Adamo, J. Jaramillo, R. Gomperts, R. E. Stratmann, O. Yazyev, A. J. Austin, R. Cammi, C. Pomelli, J. W. Ochterski, P. Y. Ayala, K. Morokuma, G. A. Voth, P. Salvador, J. J. Dannenberg, V. G. Zakrzewski, S. Dapprich, A. D. Daniels, M. C. Strain, O. Farkas, D. K. Malick, A. D. Rabuck, K. Raghavachari, J. B. Foresman, J. V. Ortiz, Q. Cui, A. G. Baboul, S. Clifford, J. Cioslowski, B. B. Stefanov, G. Liu, A. Liashenko, P. Piskorz, I. Komaromi, R. L. Martin, D. J. Fox, T. Keith, M. A. Al-Laham, C. Y. Peng, A. Nanayakkara, M. Challacombe, P. M. W. Gill, B. Johnson, W. Chen, M. W. Wong, C. Gonzalez, and J. A. Pople, *GAUSSIAN 03*, REVISION B.05 (Gaussian, Inc., Pittsburgh PA, 2003).
[13] A. D. Becke, J. Chem. Phys. **98**, 5648 (1993); C. Lee, W. Yang, and R. G. Parr, Phys. Rev. B **37**, 785 (1988).
[14] J. P. Perdew, K. Burke, and M. Ernzerhof, Phys. Rev. Lett. **77**, 3865 (1996).
[15] F. A. Hamprecht, A. J. Cohen, D. J. Tozer, and N. C. Handy, J. Chem. Phys. **109**, 6264 (1998).
[16] R. K. Kremer, Appl. Phys. A: Solids Surf. **56**, 211 (1993).
[17] J. B. Foresman and AEleen Fischer, *Exploring Chemistry With Electronic Structure Methods: A Guide to Using Gaussian*, 2nd Ed. (Gaussian, Inc., Pittsburgh, 1996), pp. 63–64.
[18] E. Osawa and K. Honda, Fullerene Sci. Technol. **4**, 939 (1996).
[19] K. Esfarjani, Y. Hashi, J. Onoe, K. Takeuchi, and Y. Kawazoe, Phys. Rev. B **57**, 223 (1998).
[20] K. A. Wang, Y. Wang, P. Zhou, J. M. Holden, S. L. Ren, G. T. Hager, H. F. Ni, P. C. Eklund, G. Dresselhaus, and M. S. Dresselhaus, Phys. Rev. B **45**, 1955 (1992).
[21] B. Burger, J. Winter, and H. Kuzmany, Z. Phys. B: Condens. Matter **101**, 227 (1996).